

Frascati, October 22, 2002

Note: **MM-33****THE OCTUPOLES OF THE DAΦNE MAIN RINGS**

*B. Bolli, S. Ceravolo, M. Incurvati, F. Iungo, C. Ligi, M. Marchetti, M. Paris,  
M. Preger, A. Reali, C. Sanelli, F. Sardone, F. Sgamma, M. Troiani*

**1. Introduction**

Eight octupoles have been built by SIGMA-Phi, and three of them are now installed on each Main Ring, with the purpose of compensating the octupole non-linearities introduced by a decapole term in the wiggler field [1]. The following table summarizes the design parameters of the magnet. Due to lack of time between delivery and installation, only one magnet has been measured, both with the Hall Probe and Rotating Coil systems.

Table 1 - Nominal Design Parameters

Magnetic length	mm	100
Bore radius	mm	50
Excitation current	A	117.4
Turns per pole		33
Gradient ( $\partial^3 B / \partial x^3$ )	T/m <sup>3</sup>	17000
Integrated gradient	T/m <sup>2</sup>	1700
Field at pole tip	T	0.354
Maximum allowable mechanical length	mm	160
Copper conductor size	mm <sup>2</sup>	5 x 5
Cooling hole diameter	mm	3
Current density	A/mm <sup>2</sup>	6.88
Total power dissipation	W	1300
Water circuits per coil in parallel		2
Water flow per magnet	l/min	1.24
Pressure drop per circuit	atm	5.9
Water temperature rise	°C	15

Figure 1 shows a picture of the octupole magnet.

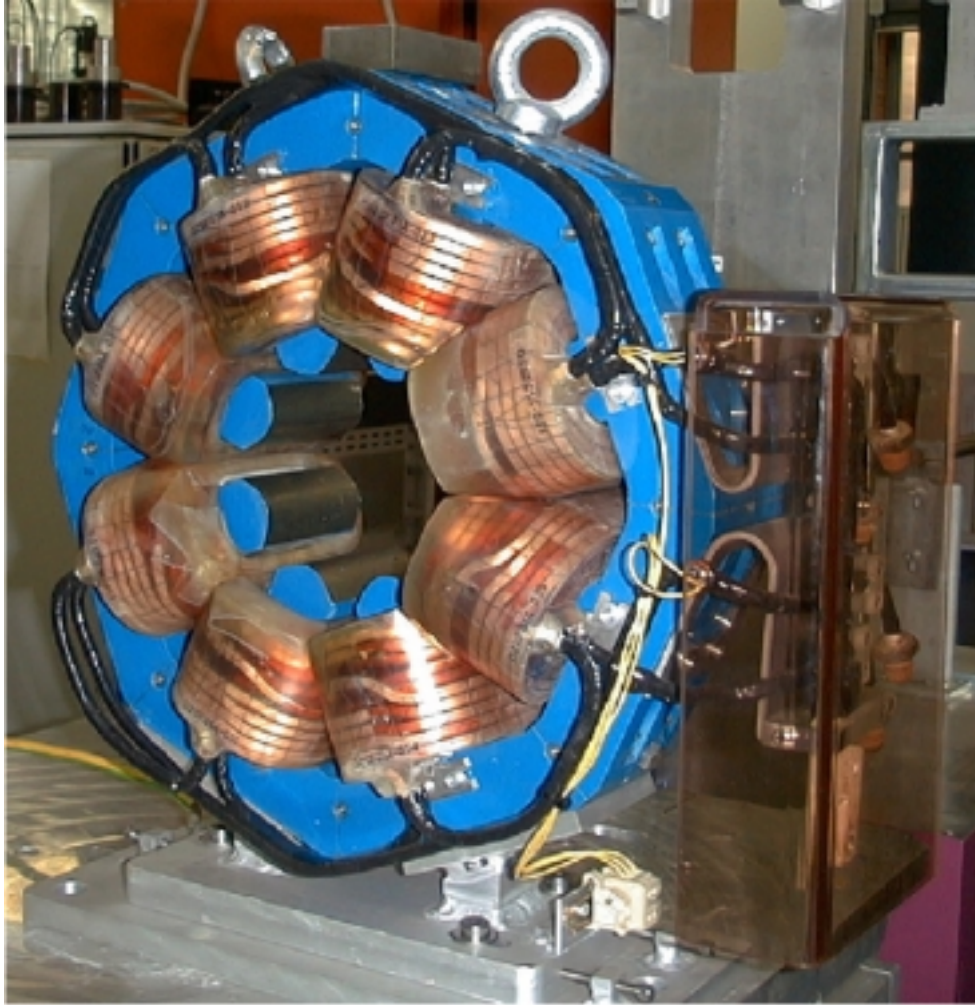


Figure 1 – The Octupole magnet

## 2. Electrical measurements

The resistance of the octupole magnet coils was measured by means of a micro-ohm-meter (AOIP mod. OM 20) at room temperature. The measured value was:

$$R = 86.7 \text{ m}\Omega @ 20 \text{ }^\circ\text{C}.$$

The same measurement was accomplished using the Volt-Ampere method and the following data were measured:

$$V = 11.15 \text{ V @ } 117.3 \text{ A, corresponding to } 95 \text{ m}\Omega.$$

This value is consistent and in good agreement with the previous one taking into account the magnet coil temperature increase, as described below.

The inductance and resistance of the octupole magnet were also measured by means of a LCR meter (HP 4248 A) at different frequencies. The results are very similar and are reported in Fig. 2.

The corresponding dc values can be extrapolated from these data. They are consistent with the measured and design data.

Thermal measurements were also accomplished at the nominal current (117.4 A) and a temperature increase of about 18.5 °C was measured under a pressure drop of 5.6 bar, that is a little less than the design value, but in any case in very good agreement with the values reported in Table 1.

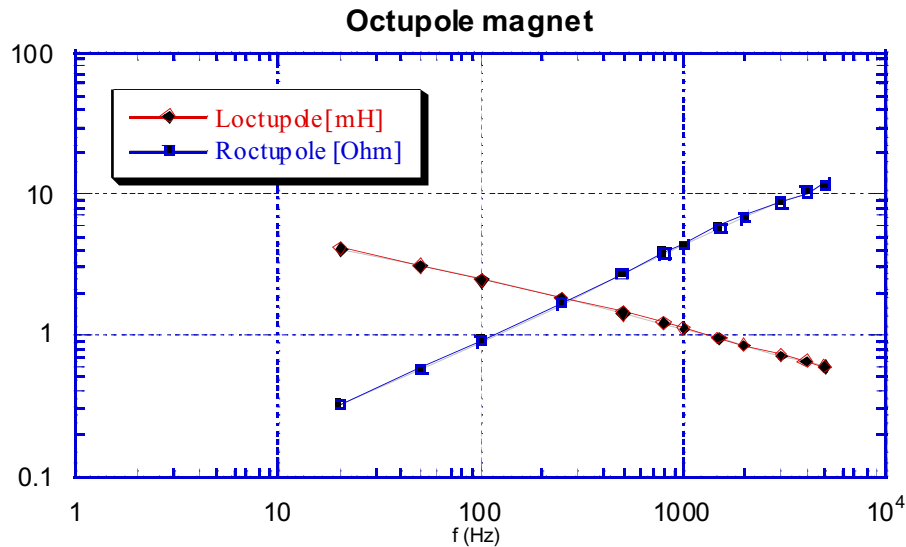


Figure 2 – Resistance and Inductance versus frequency of the Octupole magnet

### 3. Measurement with the rotating coil

The measurements have been performed by means of the coil used for the quadrupoles, modifying the acquisition software to set the octupole term as the main field component. The integrated gradient has been found to be 1649 T/m<sup>2</sup>  $\approx$  3% smaller than the nominal value at the nominal current of 117.4 A.

Table 2 shows the integrated gradient, the average absolute value of the field deviation and the contributions of the most important harmonics on a circle of 30 mm diameter. All values are scaled by the proper power of the different harmonics to this diameter from the original values measured at the coil radius of 49 mm. Figure 3 shows the behaviour of the relative deviation from the ideal octupole field versus the azimuthal angle.

Table 2 - Integrated gradient, average deviation from ideal octupole and relative higher harmonic contributions to the field at 30 mm.

Integrated third derivative (T/m <sup>2</sup> )	1649
$\langle  \Delta B/B  \rangle$ @ 30 mm (%)	0.15
10-pole @ 30 mm (%)	0.08
12-pole @ 30 mm (%)	0.11
14-pole @ 30 mm (%)	0.05
16-pole @ 30 mm (%)	0.01
18-pole @ 30 mm (%)	0.01
20-pole @ 30 mm (%)	0.01
22-pole @ 30 mm (%)	0.00
24-pole @ 30 mm (%)	0.10

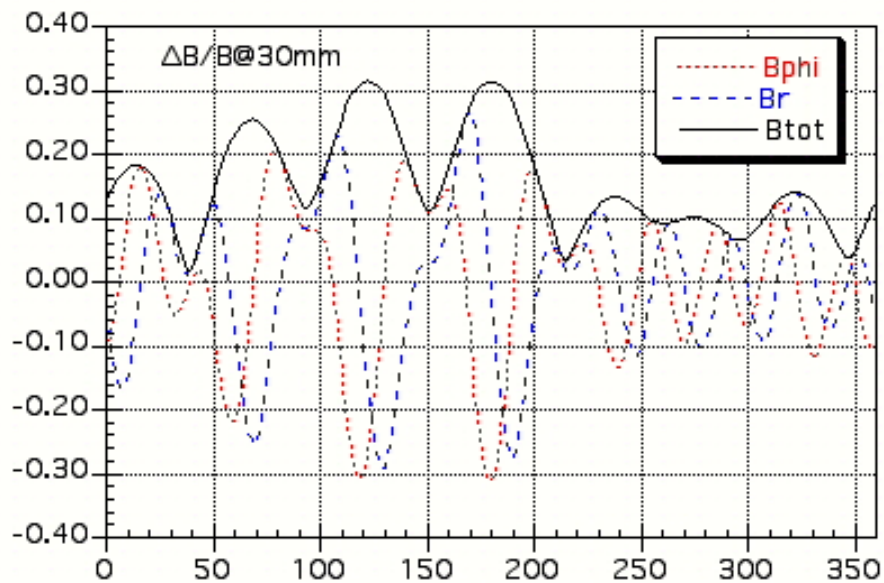


Figure 3 - Relative deviation from ideal octupole field @ 30 mm from magnet axis @117.4 A  
(Small dots = azimuthal component; large dots = radial component, full line = absolute field)

### 3. Excitation curve

The vertical component of the field has been measured as a function of the excitation current with the Hall probe placed on the horizontal symmetry plane of the magnet at a distance of 30 mm on both sides with respect to the magnet center. Figure 4 shows the result of the measurement. The slight asymmetry between the two sides is compatible with the uncertainty on the position of the sensitive part of the Hall probe inside the probe assembly and the very steep slope of the field. A slight saturation takes place above 100A.

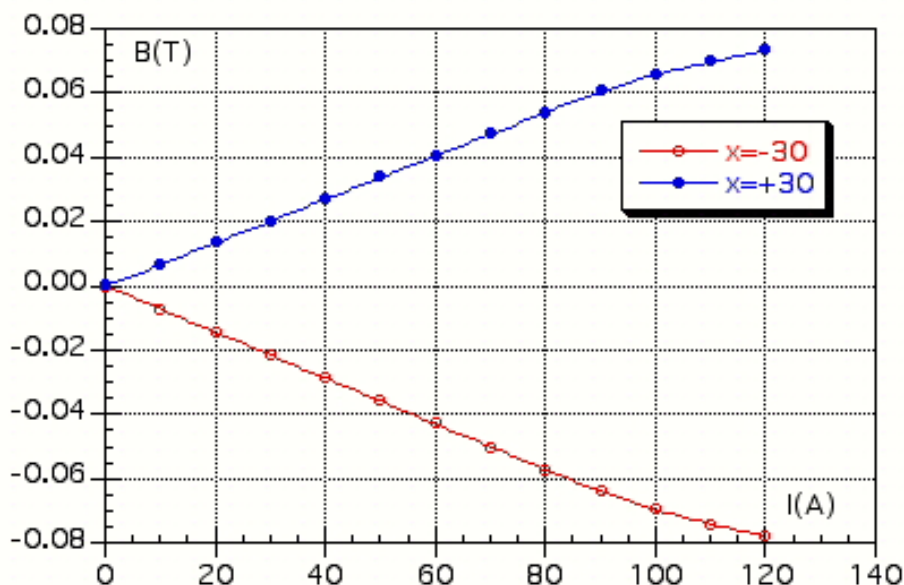


Figure 4 - Vertical field component at  $\pm 30$  mm from magnet axis versus excitation current

#### 4. Field at magnet center

The vertical component of the field has also been measured in small steps along a straight line perpendicular to the magnet axis at the magnet center, and its behaviour is shown in Fig. 5.

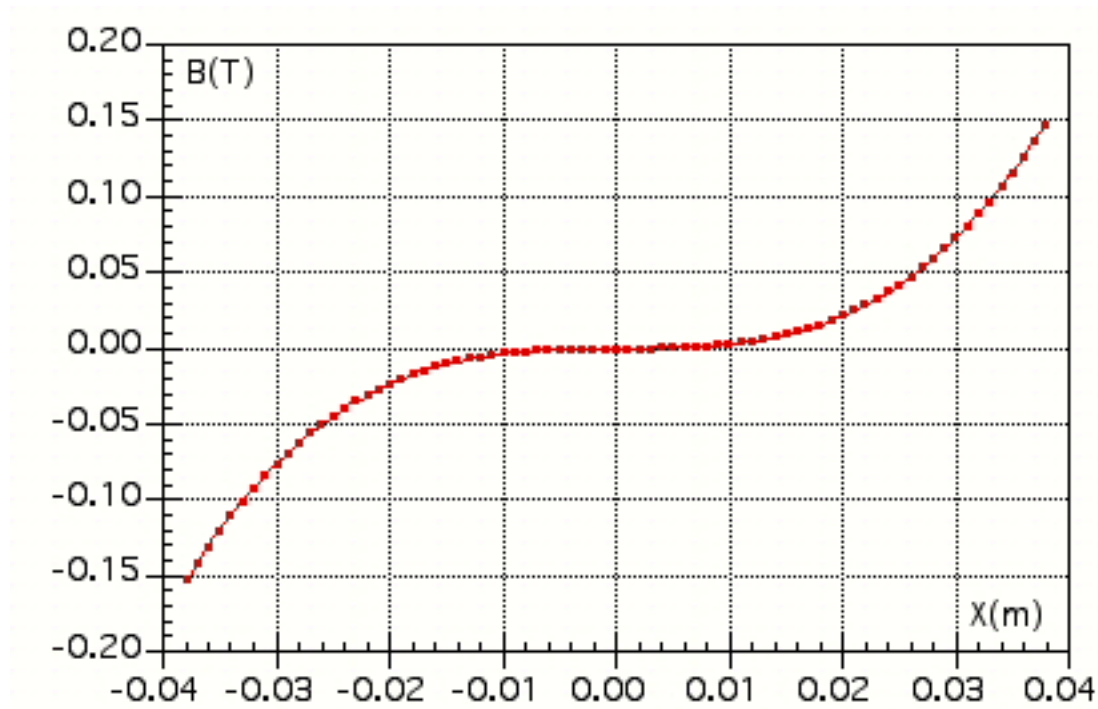


Figure 5 - Vertical field component versus horizontal position w.r.t. magnet center@117.4A

A polynomial fit to the measured points gives:

$$B_y(X) = 2722.4 X^3 - 1.855 X^2 + 0.035 X - 5.5 \times 10^{-5} \quad (B \text{ in Tesla, } X \text{ in meters})$$

The coefficient of the third order term is  $\approx 4\%$  smaller than the design value.

#### 5. Longitudinal scans

The vertical component of the field has been measured on the horizontal and vertical symmetry planes along the magnet axis and along straight lines parallel to it in order to find out the magnetic length and the dependence of the field integral on the horizontal distance from the center.

All measurements have been performed at the nominal current of 117.4 A, although the magnet is slightly saturating at that current. Figure 6 shows the result of the measurement performed on the horizontal plane, while Figure 7 is the same in the vertical plane.

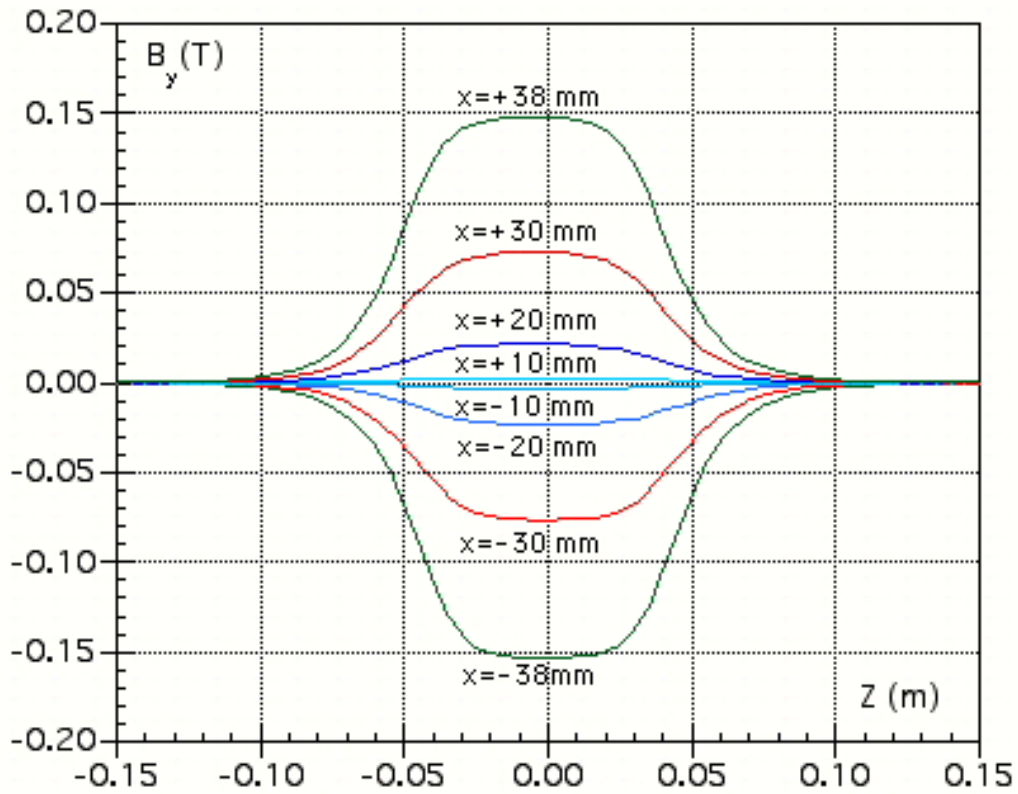


Figure 6 - Behaviour of the vertical field component along straight lines parallel to the quadrupole axis on the horizontal symmetry plane

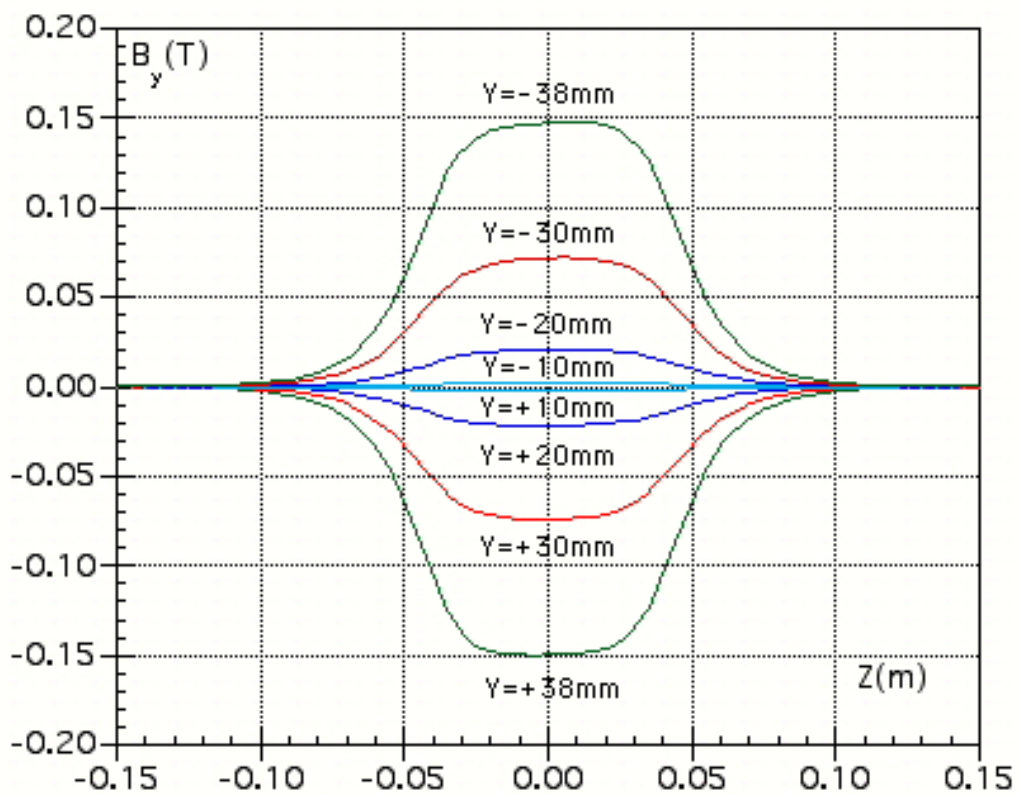


Figure 7 - Behaviour of the vertical field component along straight lines parallel to the quadrupole axis on the vertical symmetry plane

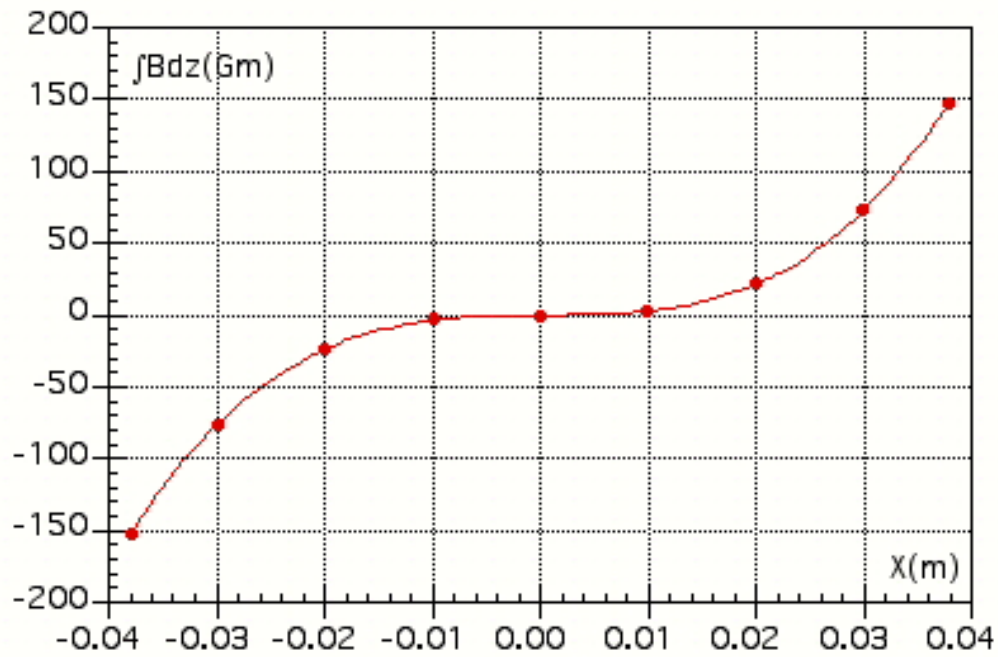


Figure 8 - Field integral versus position in the horizontal plane

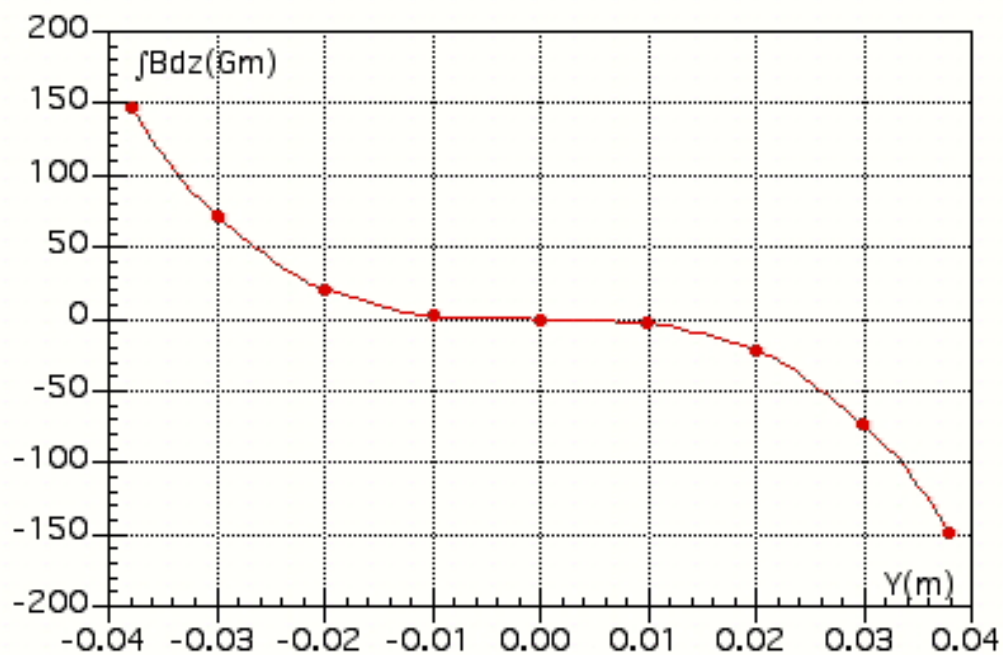


Figure 9 - Field integral versus position in the vertical plane

Figures 8 and 9 show the field integrals taken over each longitudinal scan. The measured points can be fitted with a third order polynomial obtaining

$$\int B_y dz = 270.8 X^3 - 0.174 X^2 + 0.053 X - 4.6 \times 10^{-6} \quad (\int B_y dz \text{ in Tm, } X \text{ in meters})$$

$$\int B_x dz = -272.5 Y^3 + 0.694 Y^2 + 0.027 Y + 6.3 \times 10^{-6} \quad (\int B_x dz \text{ in Tm, } Y \text{ in meters})$$

## **4. Conclusions**

The results of the measurements performed on one of the eight octupoles built for the DAFNE Main Rings have been presented. The measured gradient is smaller than the result of magnetic codes by few percents. The magnet exhibits a slight saturation above 100A, the maximum operating current being 120 A. The magnetic measurements with the Hall probe appear sometimes slightly asymmetric but, taking into account that the sensitivity to misalignments increases rapidly with the order of multipole, they are still satisfactory. The measurement with the rotating coil shows that the average field error is small, the most important higher order contributions coming from the 12-pole and 24-pole.

## **References**

- [1] M. Preger, private communication.